

MUWA: Multi-field Universal Wheel for Air-land Vehicle with Quad Variable-pitch Propellers

Koji Kawasaki, Moju Zhao, Kei Okada and Masayuki Inaba

Abstract— This paper presents a multi-field universal vehicle that is able to work at land, sea and air. The vehicle consists of a quad-copter with variable-pitch propellers that enable the vehicle to stand on the ground at a given tilt angle, roll on the ground like a wheel, and float and move on the water, in addition to flying like a conventional quad-copter. This article clarifies the behavioral objectives, structural design, basic control mechanism of the ring-shaped robot, and examples of 3D measurements.

I. INTRODUCTION

Recently, research on flying robots has attracted attention, especially for information collection at disaster sites [1]. However, these robots only fly in the horizontal direction, so that a minimum flat gap is necessary and only investigate from the sky, whereas an actual disaster site that includes indoor spaces and a cluttered environment requires a robot that can pass through narrow spaces such as half-open doors. This paper describes the development of a flying robot for multi-field use including land, sea and air with a ring-shaped quad-copter with variable-pitch propellers (Fig.1). This robot has the following three action modes. (i) flying mode with bilateral (horizontal and inverted) flight, (ii) boat mode for moving on the water utilizing the ring-shaped molded material as a body, and (iii) mono-wheel mode for rolling on the ground like a standing wheel. The robot also has a 3D measurement function, which is a combination of these three modes. Measurement function has attitude control with three degree of freedom on the ground by standing at a given angle and rotating (Fig.16).

Research into quad-copters has been developed recently, particularly in the fields of aggressive maneuvering [2][3][4] and autonomous flight control [5]. Despite the achievement of full control of quad-copters, issues of locomotion at disaster site still remain. The biggest issue is for robots to be able to pass through a vertical gap. Flying objects such as helicopters, including quad-copters, require a rotary face in the horizontal direction, and thus require a minimum flat space. Therefore, moving outdoors and large room pose no problems, while passing through a tilted space created by obliquely collapsed walls, or entering through half-opened door is difficult. In addition, a quad-copter, which cannot glide like an airplane, consumes energy while hovering, and are thus unsuitable for long-term measurement. If cameras or sensors are mounted to measure the layout of disaster areas and obtain photo information, a separate actuator is needed

to control the camera angle to obtain information from the desired direction; even if the robot body can be made small and light, adding a gimbal system for the camera and sensor increases the size and makes miniaturization difficult and results in a payload that necessitates a larger battery [6][1]. Also, when landing on areas that are not flat, such robots can fall on to their side and turn upside down, and are unable to recover from those positions.

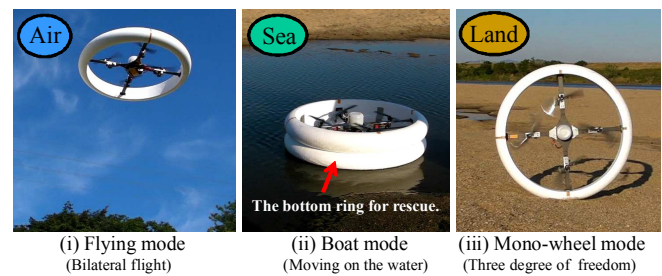


Fig. 1. Multi-field (air, sea, land) robot



Fig. 2. Example of mono-wheel mode in the field in a disaster. The robot is able to pass through narrow vertical-diagonal gaps with an inclined rolling motion.

II. DESIGN OF MUWA WITH QUAD VARIABLE-PITCH PROPELLERS

In order to realize a robot that is able to work at land, sea and air, we have developed a robot with ring-shaped polystyrene foam body to enable it to work at land, sea and air. The robot can move on land and float on water. The main characteristics of this robot is the novel motion of the mono-wheel mode on land, and the ability to remain tilted at any angle, turn while keeping its orientation, and pass through the narrow vertical-diagonal gaps with the inclined rolling motion shown in Fig.2. To control the attitude, we introduced variable pitch mechanism [7][8][9]. Inverse flight control that enables quadcopters to fly loops have been reported [10].

Today, anyone can easily design a flying robot. The flight attitude control can be classified into two types based on the quad-copter propeller mechanism: one with fixed-pitch propellers where the motor speed is used control attitude, and one with variable-pitch propellers where the propeller pitch

K. Kawasaki, M. Zhao, K. Okada and M. Inaba are with Department of Mechano-Infomatics, The University of Tokyo, 7-3-1 Hongo, Bunkyo-ku, Tokyo 113-8656, Japan kawasaki@jsk.t.u-tokyo.ac.jp

is varied to control lift. We developed the robot with variable-pitch propellers that has various modes. The concept of mono-wheel mode enabled by variable-pitch rotors is shown in Fig.3. Another mechanism of achieving attitude control is to use fixed-pitch propellers and controlling motor speed. Table.I shows a comparison of variable-pitch and fixed-pitch. A variable-pitch propeller mechanism in this robot is a complex structure, but has high-performance response for mobility (A). In addition, the robot realized inverted flight with negative lift with variable pitch (B). In boat mode, it is not necessary to control the propeller pitch angle; however, standing upright on water is impossible without the variable-pitch control of mono-wheel mode (C). In this new approach to using variable pitch, we have devised a quad-copter that can stand on the ground and roll freely with three degree of freedom (D). By combining the tornado motion described in Section V, in which the quad-copter can rotate in place at a given angle, with sensors, the quad-copter can be used to take 3D measurements of the surroundings including walls, ceilings, and floors (E). Compared with the conventional methods, in which complicated actuators are attached between the sensor and body, this new motion is able to accomplish the same objective just by rotating itself. This is a novel aspect of this work (F).

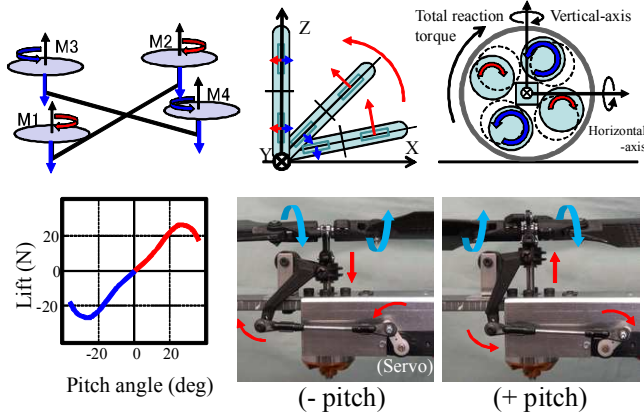


Fig. 3. Concept of mono-wheel mode enabled with variable pitch. Lift characteristics vs. pitch angle. In order to upright the zero lift at zero degrees pitch, angle is an important factor. Variable-pitch module. Individually controls the pitch angle of each propeller with actuators to seamlessly between positive and negative angles. With this variable pitch, the quad-copter is able to stand up from the ground and roll on the ground.

TABLE I
FEATURE OF THIS ROBOT WITH VARIABLE PITCH

Mode	Prototype development (Variable-pitch)	Fixed-Pitch
Flying	(A)High response (B)Bilateral flying	Single-sided flying only
Boat	(C)Motion on water	Motion on water
Mono-wheel	(D)3DOF (E)Surroundings (F)No actuator	Motion on water
Fail safe (Unimplemented)	Auto-rotation	not possible

III. CONTROL METHODS FOR GROUND LOCOMOTION

The most important issue of this study is to achieve control in mono-wheel mode. Because of the ground reaction force,

the control of the mono-wheel mode is different from flight attitude control. During flight, there is a balance between gravity and vertical lift, so the control theory is akin to a zero gravity state. In contrast, when there is contact with the ground, gravity compensation control is required with the fulcrum at the point of contact with the ground. The relationship between the forces for attitude control for a given tilt angle in the resting state are shown in Fig.4. Equations (1) and (2) show the force balance. Equation (3) shows the torque balance (3). When Equations (1) to (3) are solved, Equations (4) to (6) are obtained.

$$f_a + f_b + f_c \cos \theta = m g \cos \theta + \mu f_c \sin \theta \quad (1)$$

$$m g \sin \theta = f_c \sin \theta + \mu f_c \cos \theta \quad (2)$$

$$r \cdot (f_a - f_b) - R \cdot f_c \cdot \cos \theta + \mu \cdot R \cdot f_c \cdot \sin \theta = 0 \quad (3)$$

Now, f_a and f_b are the forces resulting from the lift exerted by the propellers. f_a refers to those components above the rolling axis, while f_b refers to those force components below the rolling axis. f_c is the force component of the ground reaction force that applies a rotational torque on the horizontal axis.

$$f_a = \frac{g m \mu \sin(\theta)^2 (R - r) - g m \cos(\theta) \sin(\theta) R - g m \mu r \cos(\theta)^2}{2 r \sin(\theta) + 2 \mu r \cos(\theta)} \quad (4)$$

$$f_b = \frac{g m \mu \sin(\theta)^2 (R + r) - g m \cos(\theta) \sin(\theta) R + g m \mu r \cos(\theta)^2}{2 r \sin(\theta) + 2 \mu r \cos(\theta)} \quad (5)$$

$$f_c = \frac{g m \sin(\theta)}{\sin(\theta) + \mu \cos(\theta)} \quad (6)$$

It is necessary to balance the lift from the four propellers with gravity to stay at a given tilt angle. The force of the ground point is only the gravity component in these equations. In addition, the coordinates of four propellers change constantly during rolling. In other words, we think that this purpose can be achieved if the gravity compensation control for balancing is carried out in all attitude states. Fig.4 shows gravity compensation in the standing posture in mono-wheel mode. It is necessary to convert from the instruction coordinates (ROLL, PITCH, YAW) based on the upright position in mono-wheel mode to the $roll_{out}$, $pitch_{out}$, and yaw_{out} coordinate system used for control in the flight mode. If the metaphor for riding a motorcycle is used to describe mono-wheel mode, the steering is the YAWaxis (yaw_{in}), left and right tilt is the ROLLaxis ($roll_{in}$) and the throttle (yaw_{out}) is the driving force. This coordinate conversion is shown in Equations (7) to (12).

$$\cos \varphi = \frac{u}{\sqrt{u^2 + v^2}} \quad (7)$$

$$\sin \varphi = \frac{v}{\sqrt{u^2 + v^2}} \quad (8)$$

$$\cos \theta = \frac{w}{\sqrt{u^2 + v^2 + w^2}} \quad (9)$$

$$roll_{out} = \cos \varphi \cdot roll_{in} + \sin \varphi \cdot yaw_{in} \quad (10)$$

$$pitch_{out} = -\sin \varphi \cdot roll_{in} + \cos \varphi \cdot yaw_{in} \quad (11)$$

$$A = \begin{bmatrix} Servo1 \\ Servo2 \\ Servo3 \\ Servo4 \end{bmatrix} = \begin{bmatrix} 1 & 0 & 1 & -1 \\ 1 & -1 & 0 & 1 \\ 1 & 1 & 0 & 1 \\ 1 & 0 & -1 & -1 \end{bmatrix} \begin{bmatrix} CtrlCommand \\ AxisPID(Roll) \\ AxisPID(Pitch) \\ AxisPID(Yaw) \end{bmatrix} \quad (12)$$

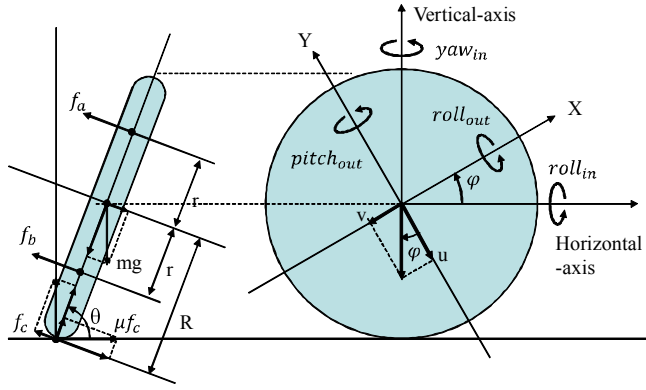


Fig. 4. Gravity compensation in the standing posture. yaw_{in} and $roll_{in}$ are commands inputted directly by the operator, while yaw_{out} and $roll_{out}$ are the desired values converted from yaw_{in} and $roll_{in}$.

IV. HARDWARE AND CONTROL SYSTEM OF MUWA

A. Hardware

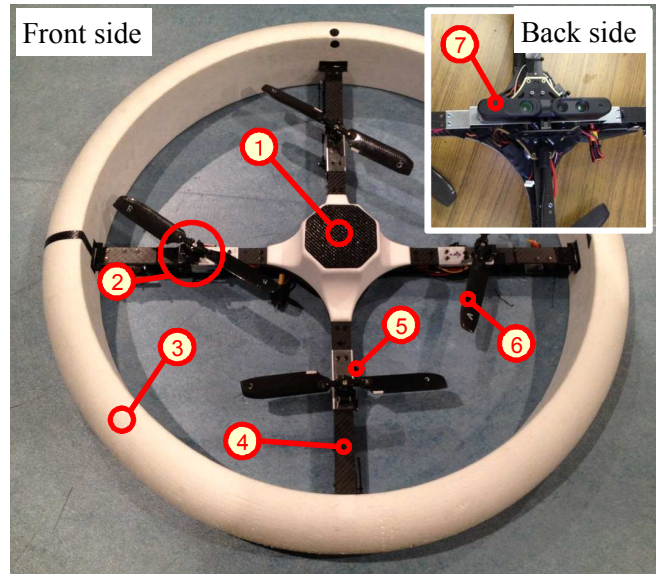
We developed the Multi-field Universal Wheel for Air-land Vehicle (MUWA), which is shown in Fig.5. This robot was built with the hope that it could be a “ring-shaped robot of dreams, active in disaster relief”. This robot is equipped with various sensors and an Arduino microcontroller board shown in the attitude control unit box in Fig.6. The pitch angle is controlled with a high-speed servo, and can be changed at a rate of $3.5msec/deg$. The pitch angle can be varied up to $\pm 20^\circ$. We have achieved a very high stability in attitude control with this high-speed response. There are several reports on the mono-wheel control using the center of gravity and inertial movement [11][12][13], however our robots were novel in that they achieved this mode using wind.

B. Control system

This section describes the attitude control model for MUWA. First, the block diagram for the overall attitude control is shown in Fig.7. The system has a feedback control for the attitude angle based on a G-sensor, and is equipped with feed-forward control for gravity compensation. The block diagram for PID control in each axis-ROLL, PITCH, and YAW-is shown in Fig.8. Selector switch leading to the Estimate Attitude blocks in the block diagram are for the switching between mono-wheel mode and flight mode. The horizontal-to-standing mode switch allows the quad-copter to rise from a horizontal posture to a standing posture.

V. BASIC MOTIONS AND EXPERIMENTS

The following items are measured as a basic motion check of the robot. The following results focus on a new function, namely mono-wheel motion. Flying function and motion on water are measured, however, they are not very different from existing technology. The measurement results for mono-wheel motion are explained, because it is a novel function. Attitude was measured by mounting a wireless IMU in the center of the body of the MUWA. The IMU sensors



Specifications of MUWA		
Dimension	Body ring outer diameter	910 mm
	Body ring inner diameter	700 mm
	Body thickness	120 mm
	Total weight	2.1 kg
Motor	Motor output	336 W
	Motor KV	1100 rpm/V
	Maximum speed	5400 rpm
Variable-pitch propeller	Propeller diameter	305 mm
	Pitch angle width	20 deg
	Pitch variable speed	3.5 ms/deg
	Propeller lift	11.1 N/propeller
	Total lift	44.4 N

Fig. 5. MUWA: Multi-field Universal Wheel Air-land Vehicle 1) Attitude control unit box, 2) Variable-pitch propeller module, 3) Ring-shaped polystyrene foam(specific gravity = $0.016g/cm^2$), 4) CFRP honeycomb frame ($t = 5mm, 230g$), 5) Servo actuator($0.07sec/60^\circ$), 6) CFRP propeller blade, 7) Xtion:Optical depth sensor for 3D measurement & Digitizing.

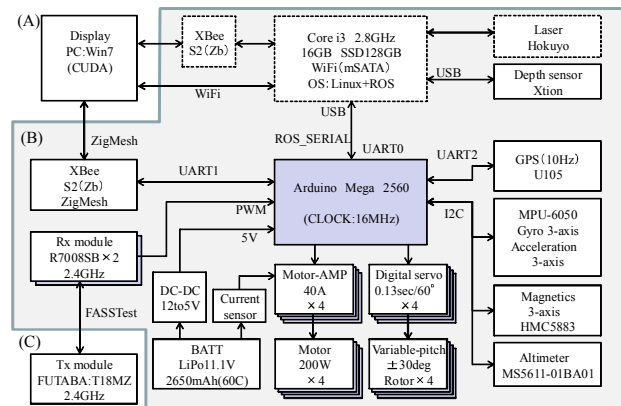


Fig. 6. Overall hardware architecture of MUWA. (A)Grand station. (B)Attitude control unit box(Fig.5-1). (C)Radio control transmitter.

can output 3-axis acceleration, 3-axis angular velocity, 3-axis geomagnetism, and 3-axis attitude angle. The attitude control is autonomous, but the motion instructions are given by remote control. The motion instructions are given by a wireless controller that transmits instructions on acceleration,

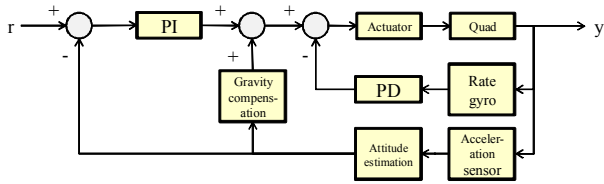


Fig. 7. Block diagram of attitude control configuration. Quad and Actuator are plant outputs, PD is an inner-loop controller.

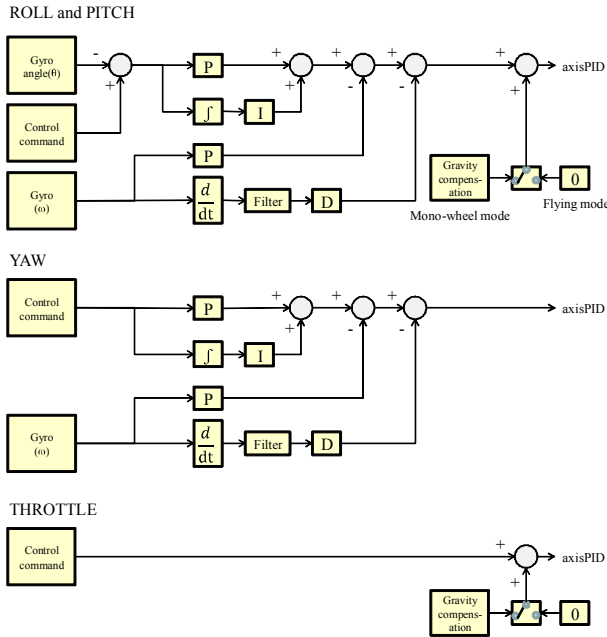


Fig. 8. Block diagram for controlling attitude in each axis

turns, and tilt angle.

A. Flying Mode Control

Fig.9 shows the measurement result of horizontal stability for flying control, which is a basic function of quad-copters. Generally, it flies like a quad-copter with general fixed-pitch propellers. However, it has a good response because the propeller pitch angle can be changed rapidly. Its stability is also very good. It can fly at a height of 200m, which is a considerable altitude. This is also the legal limit in Japan.

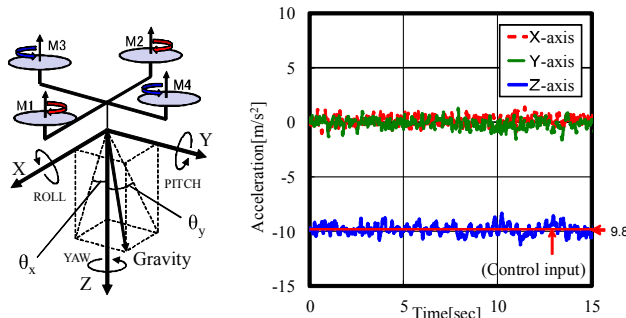


Fig. 9. Flying motion. Flying mode control coordinate (left). X, Y, and Z-axis of acceleration sensor (right).

B. Mono-Wheel Mode Control

1) *Upright and Rotating Motion:* Fig.10 shows the measurement results for rotational stability in place in the upright

position in mono-wheel mode. The attitude angle was 90° . The action steps were (1) a left turn at low speed, (2) a stop, and (3) a right turn at high speed. The results show that the deviation against vertical axis was minimal, and rotation in place was realized. The same result was also obtained at any given contact point on the wheel. For example, if a 60 degree tilt angle is specified, this angle is maintained. If an instruction is given to roll, the robot will roll on the ground maintaining the tilt.

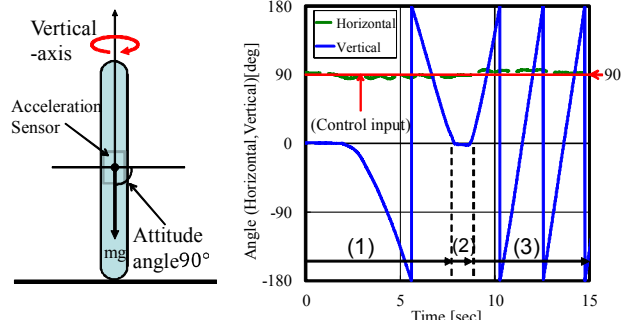


Fig. 10. Upright rotation in place. Action steps: (1) Left turn at low speed, (2) Stop, (3) Right turn at high speed.

2) *Complex Motion:* This is a sequence with a fixed point of contact on the ground. The action steps were (1) a fall in the direction of the horizontal axis, (2) 90° pivot around vertical axis, and (3) a rise to upright position. Fig.11 shows a measurement result at a given tilt angle position requested against rolling direction. Fig.12 shows the sequence. An static control is thus possible for a given tilt angle, from $0^\circ \sim 90^\circ \sim 180^\circ$ and we have verified a smooth transition from flying mode to mono-wheel mode.

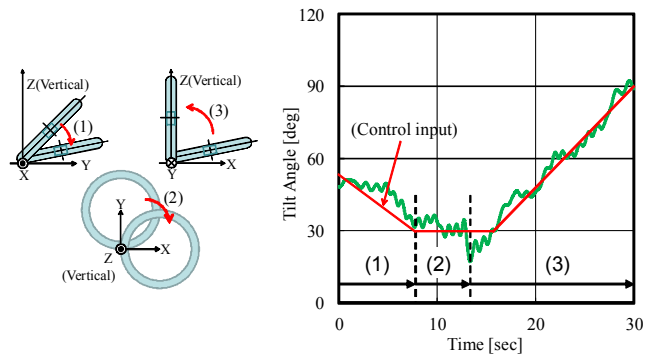


Fig. 11. Complex motion. Action steps: (1) Fall in the direction of the horizontal axis, (2) 90° pivot around vertical axis, (3) Rise to upright.

3) *Rolling Motion:* This chapter describes the movement of mono-wheel rolling. We determined how to use the motor torque reaction force, which is used for yaw control in flight, as a propulsion force. The attitude angle is 90° . The action steps are (1) rolling two turns ($4km/h$), and then (2) stopping. The acceleration in the X, Y, and Z axes during rolling is shown in Fig.13 (top). The X-Y plane (Lissajous figure) for acceleration during rolling is shown in Fig.13 (bottom). The experimental results show that the sum of squares for X-

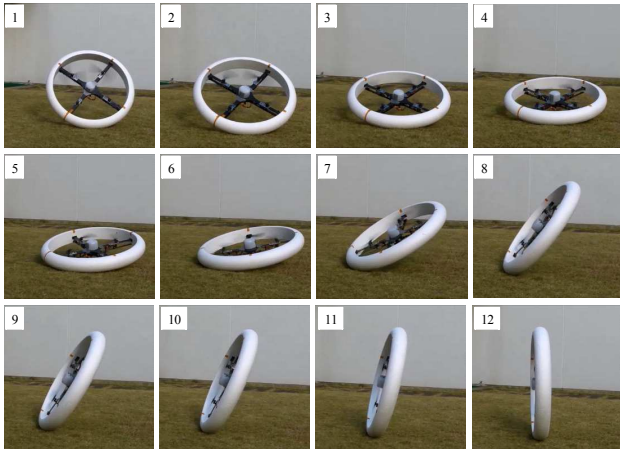


Fig. 12. Complex motion. Photo No.1 to 3 represent Action step (1), Photo No.4 to 6 represent Action step (2), and Photo No.7 to 12 represent Action step (3).

Y axis acceleration and gravitational acceleration ($9.8m/s^2$) correspond very well. As an application, it is possible to pass through a narrow, angled space by rolling at a given tilt angle as shown in Fig.2 above. Also, the direction can be freely changed without steering as shown in Fig.10.

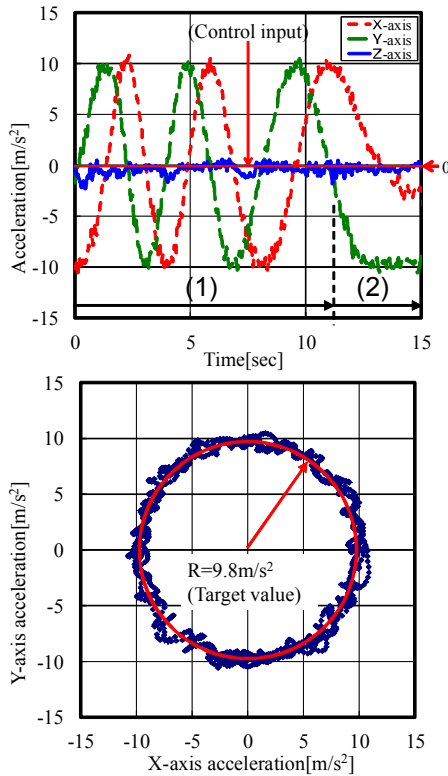


Fig. 13. Rolling motion. The action steps are (1) rolling two turns ($4km/h$), (2) Stop the rotation. Rolling with an entirely vertical attitude is the gravitational acceleration shown as a red circle in the Lissajous figure (bottom).

4) *Tornado Motion*: The robot rotates on the spot, pivoting with vertical axis, putting the main body in the center and holding the tilt of X and Y axis. We describe it as a 'tornado motion'. Fig.14 shows the motion sequence. Fig.15 shows the position measuring results for tornado motion. The

rolling angle and pitch angle are not in phase, which means the motion includes a set yaw rotation. The robot rotates on the spot, holding a 60-degree tilt on the X-Y plane. As shown in Fig.13 (bottom), for rolling with an entirely vertical attitude, the sum of squares for the measured acceleration for both the X and Y axes show a good correlation with the desired value, which is the gravitational acceleration shown as a red circle in the Lissajous figure. On the other hand, as shown in Fig.15 (bottom), while rotating on a vertical axis with an inclination of 60° , the peak values also show a good correlation with a different desired value which is $m \cdot g \cdot \cos(60^\circ) = 8.5m/s^2$.

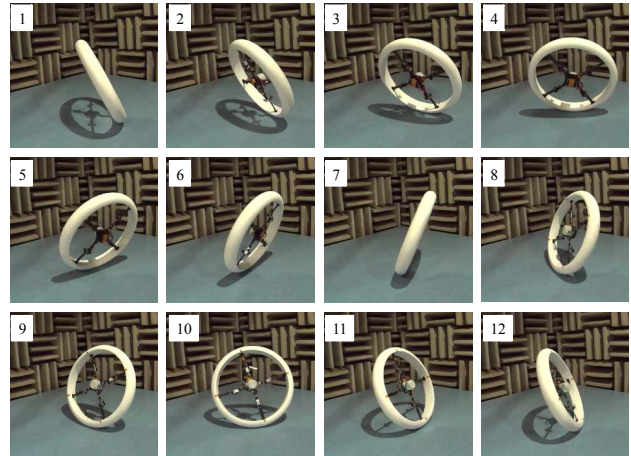


Fig. 14. Example of tornado motion: the robot rotates around a vertical axis and maintaining an X-Y tilt with the body in the center.

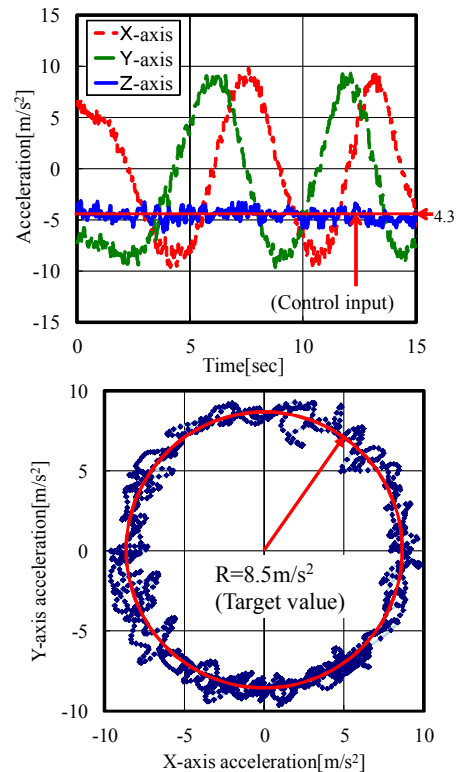


Fig. 15. Tornado motion. Rotating around the a vertical axis with the inclination of 60° ; peak acceleration is $8.5m/s^2$

C. 3D Measurement

A novel measurement function was achieved with the tornado motion. With the camera and Xtion sensors on the main body (Fig.16 (top)), photographing and measuring any direction in three dimensions are possible with the tornado motion without the installation of an additional actuator on the body. Also, the robot was used to take 3D measurements at a mock disaster site by changing the position and angle of the body. This measurements were made by remotely controlling the robot and without autonomous control. Fig.16 (bottom) shows the 3D measurements of a large motor in a narrow space surrounded by walls. These measurements were made with an Xtion (depth sensor) and PCL (Point Cloud Library). The top part of the motor was measured in flying mode, while the sides were measured in mono-wheel mode. In particular, changing the inclination angle of the body broadens the horizon. Furthermore, the outer surrounds of the room can be measured with the tornado motion. Methods [14][15] have been reported in the R&D on the creation of 3D maps using a quad-copter with a laser sensor and a camera. We referred to existing 3D measurement methods for PCL [16][17] using KinectFusion.

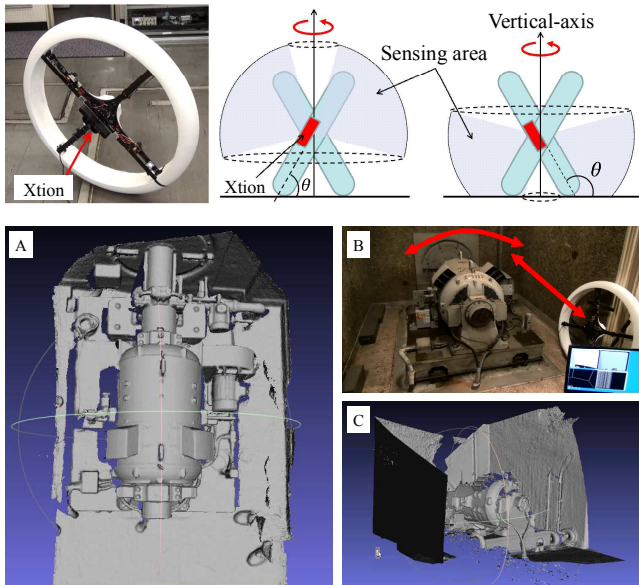


Fig. 16. 3D measurement operation using tornado motion. Xtion sensors on the main body (top left). Measurement of entire room using the tornado motion (top right). Examples of 3D measurements (bottom): 3D measurement of a large motor in a narrow space surrounded by walls. The measurements were made with a Xtion (depth sensor) and PCL (Point Cloud Library).

VI. CONCLUSIONS

We developed the “MUWA” flying robot for multi-field use including air, sea and land. It has a is ring-shaped quad-copter with variable pitch propellers. This robot has the following three action modes-flying, boat, and mono-wheel modes as well as the 3D measuring mode, which is a combination of those modes. We have checked the basic motions using an actual robot and proved the effectiveness.

We look forward to applying this robot in the field of disaster management by adding autonomous control and new actions.

REFERENCES

- [1] Michal Podhradsky. Visual Servoing for a Quadcopter Flight Control. Master’s thesis, Czech Technical University, Czechoslovakia, 2012.
- [2] Haomiao Huang, G.M. Hoffmann, S.L. Waslander, and C.J. Tomlin. Aerodynamics and control of autonomous quadrotor helicopters in aggressive maneuvering. In *2009 IEEE International Conference on Robotics and Automation (ICRA)*, pp. 3277–3282, May 2009.
- [3] D. Mellinger and V. Kumar. Minimum snap trajectory generation and control for quadrotors. In *2011 IEEE International Conference on Robotics and Automation (ICRA)*, pp. 2520–2525, May 2011.
- [4] Daniel Mellinger, Nathan Michael, and Vijay Kumar. Trajectory generation and control for precise aggressive maneuvers with quadrotors. *I. J. Robotic Res.*, pp. 664–674, 2012.
- [5] S. Bouabdallah and R. Siegwart. Full control of a quadrotor. In *2007 IEEE/RSJ International Conference on Intelligent Robots and Systems (IROS)*, pp. 153–158, November 2007.
- [6] O. Bourquardez, R. Mahony, N. Guenard, F. Chaumette, T. Hamel, and L. Eck. Image-Based Visual Servo Control of the Translation Kinematics of a Quadrotor Aerial Vehicle. *IEEE Transactions on Robotics*, Vol. 25, No. 3, pp. 743–749, June 2009.
- [7] B. Michini, J. Redding, N.K. Ure, M. Cutler, and J.P. How. Design and flight testing of an autonomous variable-pitch quadrotor. In *2011 IEEE International Conference on Robotics and Automation (ICRA)*, pp. 2978–2979, May 2011.
- [8] M. Cutler, N. Kemal Ure, B. Michini, and J. P. How. Comparison of Fixed and Variable Pitch Actuators for Agile Quadrotors. In *AIAA Guidance, Navigation, and Control Conference (GNC)*, Portland, OR, August 2011.
- [9] J. Gebauer, P. Koci, and P. Sofer. Multicopter potentialities. In *2012 13th International Carpathian Control Conference (ICCC)*, pp. 194–197, May 2012.
- [10] Mark Cutler and Jonathan P. How. Actuator constrained trajectory generation and control for variable-pitch quadrotors. In *AIAA Guidance, Navigation, and Control Conference (GNC)*, 2012.
- [11] Yangsheng Xu and S.K.-W. Au. Stabilization and path following of a single wheel robot. *IEEE/ASME Transactions on Mechatronics*, Vol. 9, No. 2, pp. 407–419, June 2004.
- [12] Tomasz Buratowski, Patryk Cielak, Mariusz Giergiel, and Tadeusz Uhl. A SELF-STABILISING MULTIPURPOSE SINGLE-WHEEL ROBOT. *JOURNAL OF THEORETICAL AND APPLIED MECHANICS*, Vol. 50, No. 1, pp. 99–118, 2012.
- [13] Y. Fujimoto and S. Uchida. Three Dimensional Posture Control of Mono-wheel Robot with Roll Rotatable Torso. In *ICM2007 4th IEEE International Conference on Mechatronics*, pp. 1–5, May 2007.
- [14] Lionel Heng, Gim Hee Lee, Friedrich Fraundorfer, and Marc Pollefeys. Real-time photo-realistic 3D mapping for micro aerial vehicles. In *2011 IEEE/RSJ International Conference on Intelligent Robots and Systems (IROS)*, pp. 4012–4019, September 2011.
- [15] Lefteris Doitsidis, Stephan Weiss, Alessandro Renzaglia, Markus Achtelik, Elias Kosmatopoulos, Y. Siegwart, Roland, and Davide Scaramuzza. Optimal surveillance coverage for teams of micro aerial vehicles in GPS-denied environments using onboard vision. *Autonomous Robots*, Vol. 33, pp. 173–188, 2012.
- [16] Richard A. Newcombe, Andrew J. Davison, Shahram Izadi, Pushmeet Kohli, Otmar Hilliges, Jamie Shotton, David Molyneaux, Steve Hodges, David Kim, and Andrew Fitzgibbon. KinectFusion: Real-time dense surface mapping and tracking. In *Mixed and Augmented Reality (ISMAR), 2011 10th IEEE International Symposium on*, pp. 127–136, October 2011.
- [17] Shahram Izadi, David Kim, Otmar Hilliges, David Molyneaux, Richard Newcombe, Pushmeet Kohli, Jamie Shotton, Steve Hodges, Dustin Freeman, Andrew Davison, and Andrew Fitzgibbon. KinectFusion: real-time 3D reconstruction and interaction using a moving depth camera. In *Proceedings of the 24th annual ACM symposium on User interface software and technology*, UIST ’11, pp. 559–568, New York, NY, USA, 2011. ACM.